


MT1-MMP and ADAM10/17 exhibit a remarkable overlap of shedding properties

Ludwig Werny¹, Antonia Grogro¹, Kira Bickenbach¹, Cynthia Bülck¹, Fred Armbrust¹, Tomas Koudelka², Kriti Pathak¹, Franka Scharfenberg¹, Martin Sammel¹, Farah Sheikhouy¹, Andreas Tholey², Stefan Linder³ and Christoph Becker-Pauly¹ 

1 Institute of Biochemistry, University of Kiel, Germany

2 Institute of Experimental Medicine, AG Proteomics & Bioanalytics, University of Kiel, Germany

3 Institute of Medical Microbiology, Virology and Hygiene, University Medical Center Eppendorf, Hamburg, Germany

Keywords

ADAM10; ADAM17; meprin; MT1-MMP; proteolysis; shedding

Correspondence

C. Becker-Pauly, University of Kiel, Institute of Biochemistry, Unit for Degradomics of the Protease Web, Otto-Hahn-Platz 9, 24118 Kiel, Germany
 Tel: +49-431-880-7118
 E-mail: cbeckerpauly@biochem.uni-kiel.de

(Received 13 January 2022, revised 20 June 2022, accepted 28 July 2022)

doi:10.1111/febs.16586

Membrane-type-I matrix metalloproteinase (MT1-MMP) is one of six human membrane-bound MMPs and is responsible for extracellular matrix remodelling by degrading several substrates like fibrillar collagens, including types I-III, or fibronectin. Moreover, MT1-MMP was described as a key player in cancer progression and it is involved in various inflammatory processes, as well as in the pathogenesis of Alzheimer's disease (AD). The membrane-tethered metalloprotease meprin β as well as a disintegrin and metalloproteinase 10 (ADAM10) and ADAM17 are also associated with these diseases. Interestingly, meprin β , ADAM10/17 and MT1-MMP also have a shared substrate pool including the interleukin-6 receptor and the amyloid precursor protein. We investigated the interaction of these proteases, focusing on a possible connection between MT1-MMP and meprin β , to elucidate the potential mutual regulations of both enzymes. Herein, we show that besides ADAM10/17, MT1-MMP is also able to shed meprin β from the plasma membrane, leading to the release of soluble meprin β . Mass spectrometry-based cleavage site analysis revealed that the cleavage of meprin β by all three proteases occurs between Pro₆₀₂ and Ser₆₀₃, N-terminal of the EGF-like domain. Furthermore, only inactive human pro-meprin β is shed by MT1-MMP, which is again in accordance with the shedding capability observed for ADAM10/17. *Vice versa*, meprin β also appears to shed MT1-MMP, indicating a complex regulatory network. Further studies will elucidate this well-orchestrated proteolytic web under distinct conditions in health and disease and will possibly show whether the loss of one of the above-mentioned sheddases can be compensated by the other enzymes.

Introduction

The maintenance of countless biological regulatory processes within an organism relies on the correct proteolysis of proteins as an irreversible posttranslational

modification. Hence, dysregulation of proteases within this well-organized network is often involved in many diseases, including neurodegeneration, cancer and

Abbreviations

AD, Alzheimer's disease; ADAM, a disintegrin and metalloproteinase; APP, amyloid precursor protein; C-term., C-terminal; DMSO, dimethyl sulfoxide; ECM, extracellular matrix; ecto., ectodomain; GAPDH, glyceraldehyde 3-phosphate dehydrogenase; IL-6R, interleukin-6 receptor; IP, immunoprecipitation; Mep, meprin; MMP2, matrix metalloproteinase 2; MT1-MMP, membrane-type-I matrix metalloproteinase; MT2, matriptase 2; PLA, proximity ligation assay; PM, plasma membrane; rec., recombinant.; sn, supernatant; TIMP, tissue inhibitor of metalloproteinase.

fibrosis [1–3]. Metzincins belong to the metalloprotease family and complex a zinc ion within their catalytic pocket to enable proteolytic activity. Members of this group are matrix metalloproteinases (MMPs), ADAMs (a disintegrin and metalloproteinases), ADAMTs (ADAMs with thrombospondin motifs) and astacins, including meprins.

As a typical type-I transmembrane protein, meprin β is involved in the shedding of manifold substrates, ranging from cytokines and their receptors like the interleukin-6 receptor (IL-6R) [4], to several components of the extracellular matrix (ECM), such as nidogen-I [5], mucin 2 [6], syndecan-1 [7] or procollagens I, III and VII [3,8–10]. Meprin β is expressed as an inactive zymogen and needs activation via tryptic proteases like trypsin [11] or tissue kallikrein-related peptidase (KLK) 5 [12], to cleave off its inhibitory pro-peptide and gain its proteolytic function. Additionally, membrane-tethered matriptase 2 (MT2) or the secreted bacterial protease Arg-gingipain (RgpB) from *Porphyromonas gingivalis* are able to activate meprin β [13,14].

Membrane-type-I matrix metalloproteinase (MT1-MMP, also known as MMP14) is one of six human membrane-bound MMPs and is transported to the plasma membrane (PM) as an active enzyme, due to the cleavage of its pro-peptide by a pro-protein convertase like furin along the secretory pathway [15]. MT1-MMP has an important role in remodelling the ECM, either by directly degrading substrates like fibrillar collagens types I–III [16,17] or by activating pro-MMP2, enabling the degradation of collagen type IV [18].

The most prominent examples of ADAM proteases are ADAM10 and ADAM17 (in the following also referred to as ADAM10/17). They are also membrane-anchored proteases, capable of ectodomain-shedding of various substrates like cell adhesion molecules, growth factors, chemokines and their receptors [19]. Interestingly, MT1-MMP, ADAM10, ADAM17 and meprin β have a shared substrate pool including fibronectin [17,20,21], IL-6R [4,22], IL-11R [23] or the amyloid precursor protein (APP) [24–28]. However, they sometimes have opposing roles in processing the same substrate. For instance, the shedding of APP can take place in different ways. ADAM10/17 are both described as α -secretases of APP, generating sAPP α and promoting the non-amyloidogenic pathway (Fig. 1A) [29]. On the contrary, meprin β cleaves APP as an alternative β -secretase, leading to sAPP β . Thereafter, the remaining membrane-stump (C99) can be further cleaved via intramembrane-proteolysis by the γ -secretase-complex, generating toxic A β fragments

(Fig. 1A) [30]. Importantly, the β -secretase activity of meprin β is restricted to its membrane-bound form, while both membrane-tethered and soluble meprin β can generate truncated fragments of APP like N-APP20 [24,25]. Recently, MT1-MMP was also described to play a role in the pathogenesis of Alzheimer's disease (AD) by proteolysis of APP. However, its function in APP pathology is pleiotropic. On the one hand, it acts as a η -secretase and directly cleaves APP, leading to a soluble APP fragment (sAPP η , also known as sAPP95) distinct from sAPP α or sAPP β (Fig. 1A) [31]. Moreover, MT1-MMP has also been described to dramatically increase C99 and A β levels, when transiently expressed in human embryonic kidney 293T (HEK 293T) cells, stably expressing APP with the familial Swedish mutation (HEK_{swe}), by a yet unknown mechanism. However, it was speculated that the membrane-stub remaining after η -cleavage (CTF-30, also known as η -CTF) could be a precursor of C99 [31]. On the other hand, the recombinant catalytic domain of MT1-MMP could also have A β -degrading activities, as seen in cell culture experiments or when incubated *ex vivo* on brain slices of transgenic AD Tg2576 mice [27].

So far, only ADAM10 and ADAM17 were shown to cleave meprin β from the PM, while meprin β itself can induce the activities of ADAM9, –10 and –17 by cleavage of their pro-peptides [32]. However, we speculated that MT1-MMP could also be part of this proteolytic web. Therefore, we addressed a possible connection between MT1-MMP and meprin β , elucidating potential mutual regulations and interactions of both enzymes. Herein, we show via cell-based *in vitro* experiments that MT1-MMP and meprin β are able to shed each other from the PM. Moreover, the shedding of meprin β by MT1-MMP is similar to the shedding by ADAM10/17 and all enzymes use the exact same cleavage site between Pro₆₀₂ and Ser₆₀₃, N-terminal of the EGF-like domain of meprin β .

Results

Co-expression of MT1-MMP and meprin β influences their substrate cleavage

As meprin β and MT1-MMP have a shared substrate pool, we first investigated whether co-expression of both proteases would lead to changes in their substrate cleavage. To exclude the effects of ADAM10/17 and to make the approach less complex, we used ADAM10 and ADAM17 deficient HEK 293T cells (HEK ADAM10/17^{-/-} cells). First, we co-transfected meprin

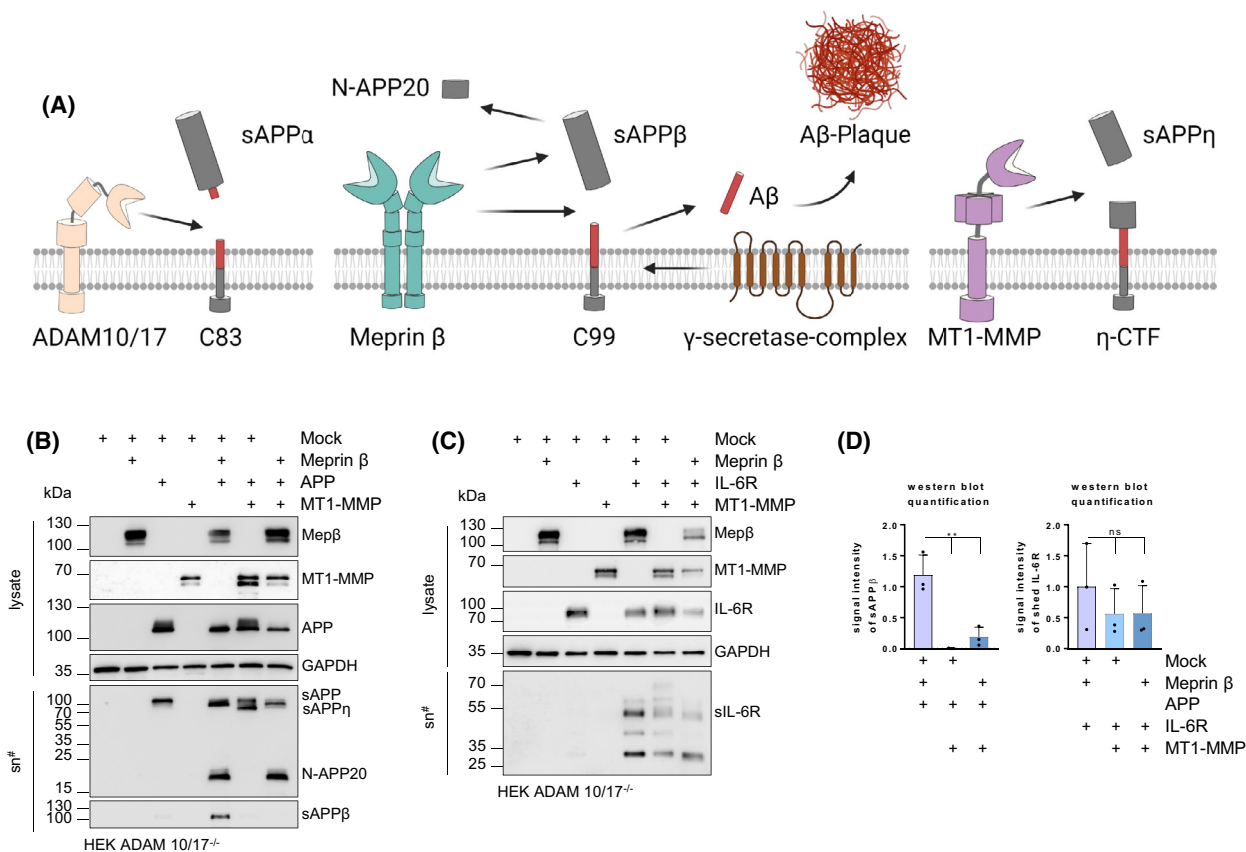


Fig. 1. Co-transfection of MT1-MMP with meprin β can influence their substrate cleavage in HEK ADAM10/17^{-/-} cells. (A) Schematic illustration of the different pathways of APP shedding. (B, C) transfection of HEK ADAM10/17^{-/-} cells with human meprin β , human MT1-MMP and human APP or human IL-6R. Immunoblotting was used to analyse cell lysates and supernatants. For detection, specific antibodies against meprin β , MT1-MMP, APP, sAPP β and IL-6R were used. GAPDH served as loading control. (D) Western blot quantification of B and C (B, C: # All supernatants were ultracentrifuged and TCA-precipitated). Mep, meprin; sn, supernatant. Data for western blot quantification represent means \pm SD, statistical analysis was performed by 1-way ANOVA, followed by Tukey's *post hoc* test from three biological replicates. * P < 0.05, ** P < 0.01, *** P < 0.001.

β and MT1-MMP together with APP in HEK ADAM10/17^{-/-} cells. Co-expression of meprin β with APP led to a clear induction of the β -secretase pathway, indicated by a strong signal for sAPP β in the ultracentrifuged supernatant (Fig. 1B). Moreover, an additional N-APP20 cleavage fragment was detectable, which is specifically generated by meprin β [25]. In contrast, co-transfection of APP with MT1-MMP generated the typical η -secretase cleavage fragment sAPP η (Fig. 1B). Interestingly, combined co-expression of MT1-MMP and meprin β together with APP, led to a strong decrease of both η - and β -cleavage, indicating a competitive activity of MT1-MMP and meprin β (Fig. 1B,D). However, N-APP cleavage seemed not to be influenced, as the intensity of the N-APP20 fragment was not altered, in comparison to APP cleavage by meprin β alone. Next, we

were interested in whether this mutual interference could also be observed for the shedding of the IL-6R. Thus, HEK ADAM10/17^{-/-} cells were co-transfected with MT1-MMP, meprin β and the IL-6R. Similar to APP, a tendency for declined shedding of the IL-6R was observed when both proteases were present, in comparison to their single-transfection with the IL-6R (Fig. 1C,D).

MT1-MMP and meprin β interact with each other

Based on the competitive cleavage activity towards APP, we were interested in whether meprin β and MT1-MMP could directly interact with each other. As both proteases are described as transmembrane proteins, we first checked their expression at the PM, using immunofluorescence microscopy. Hence, HeLa

cells were co-transfected with a pHluorin-tagged MT1-MMP construct (MT1-MMP-pH) and flag-tagged meprin β . The pHluorin-tag is a pH-sensitive variant of the green fluorescent protein (GFP) and was inserted N-terminal of the transmembrane domain of MT1-MMP and is primarily fluorescent at the extracellular pH of 7.4 [33,34]. Thus, we were able to verify the presence of MT1-MMP and meprin β at the PM, enabling possible interactions (Fig. 2A). Furthermore, cell surface biotinylation assays confirmed the existence of both proteases at the PM (Fig. 2B).

To investigate a direct interaction between meprin β and MT1-MMP we performed co-immunoprecipitation (Co-IP) experiments. Therefore, HEK ADAM10/17^{-/-} cells were transfected with meprin β and MT1-MMP. Crosswise co-immunoprecipitation of meprin β or MT1-MMP allowed the identification of the respective corresponding protease via immunoblot assays (Fig. 2C). To further prove that an interaction between MT1-MMP and meprin β was not an overexpression artefact, we performed a proximity ligation assay (PLA) with endogenous levels of both proteins. Therefore, we generated a meprin β -deficient Colo 320 cell line using CRISPR/Cas9 genome editing (Fig. 2D,E) and compared the PLA signals between these Colo 320 MEP1B^{-/-} cells and Colo 320 wild-type cells with different antibody combinations. On the one hand, we used antibodies against the ectodomains of MT1-MMP and meprin β (Fig. 2F,G); on the other hand, we permeabilized the cells and used antibodies against the C-terminal parts of MT1-MMP and meprin β (Fig. 2H,I). In both cases, clear PLA signals were detectable in Colo 320 wild-type cells in comparison to Colo 320 MEP1B^{-/-} cells (Fig. 2F-I). Hence, a direct interaction between MT1-MMP and meprin β is also possible with endogenous expressed proteins.

MT1-MMP and meprin β shed each other

Next, we investigated the effects of different inhibitors on the endogenous shedding of meprin β in Colo 320 cells. The hydroxamate inhibitors GI254023X (ADAM10) and GW208264X (ADAM10/17) as well as the broadband metalloproteinase inhibitor marimastat led to a clear reduction of soluble meprin β in the supernatant of Colo 320 cells, whereas actinonin (meprin, ADAM10/17) and an inhibitory antibody against the ectodomain of MT1-MMP (Mab3328) did not alter the shedding of meprin β (Fig. 3A).

On the contrary, we performed overexpression experiments and transfected HEK 293T cells with MT1-MMP and meprin β and investigated possible direct proteolytic events. Surprisingly, we found that soluble meprin β fragments were induced, when MT1-MMP was co-transfected with meprin β (Fig. 3B). Moreover, meprin β seemed to be capable of cleaving MT1-MMP from the PM, as corresponding soluble MT1-MMP fragments were detectable in the supernatant. As a proof of direct proteolytic interaction, we could show that the inactive meprin β variant E153A was not able to induce MT1-MMP shedding (Fig. 3B).

Since the shedding of meprin β in HEK 293T cells was induced when MT1-MMP was present, we wanted to elucidate whether MT1-MMP could interfere with the activity of ADAM10/17. Therefore, we transfected HEK ADAM10/17^{-/-} cells with MT1-MMP and ADAM10 or ADAM17. Interestingly, the autocatalysis of both ADAM proteases seemed to be affected by co-transfection with MT1-MMP, as indicated by reduced signals of soluble ADAM fragments in immunoblots (Fig. 3C) and less activity of soluble ADAMs in the corresponding supernatants (Fig. 3D). However, no explicit additional shedding events between MT1-MMP and ADAM10/17 were detectable (Fig. 3C).

Fig. 2. Interaction of meprin β and MT1-MMP. (A) HeLa cells were transfected with flag-tagged meprin β and MT1-MMP-pH and immunofluorescence microscopy images were captured (scale bars, 10 μ m). DAPI is displayed in blue, meprin β in red and MT1-MMP in green. MT1-MMP was pHluorin-tagged, for detection of meprin β , a flag antibody was used. (B) Cell surface biotinylation of HEK ADAM10/17^{-/-} cells transfected with human meprin β and human MT1-MMP. Immunoblotting was used to analyse the lysate controls and the biotin pull-down. For detection, specific antibodies against meprin β and MT1-MMP were used. GAPDH and pan-Cadherin served as controls. (C) HEK ADAM10/17^{-/-} cells were transfected with human meprin β and human MT1-MMP, followed by pulling on meprin β or MT1-MMP respectively. For detection, specific antibodies against MT1-MMP and meprin β were used. GAPDH served as loading control. (D) Genotype PCRs of Colo 320 and Colo 320 MEP1B^{-/-} cells. Agarose gel was used to visualize meprin β -specific signals. (E) Immunoblotting of lysates of Colo 320 and Colo 320 MEP1B^{-/-} cells. For detection, a specific antibody against meprin β was used. GAPDH served as loading control. (F) Proximity ligation assay of Colo 320 and meprin β -deficient Colo 320 cells (Colo 320 MEP1B^{-/-}) with antibodies against the ectodomains (ecto.) of MT1-MMP and meprin β . DAPI is displayed in blue, PLA signals in red (scale bars, 5 μ m). (G) Quantification of the PLA signals of the immunofluorescence images of F. (H) PLA of permeabilized Colo 320 and Colo 320 MEP1B^{-/-} cells with antibodies against the C-terminal parts (C-term.) of MT1-MMP and meprin β . DAPI is displayed in blue, PLA signals in red (scale bars, 5 μ m). (I) Quantification of the PLA signals of the immunofluorescence images of H. IP, immunoprecipitation; MEP, meprin; PLA, proximity ligation assay. Data for immunofluorescence quantification represent means \pm SD, statistical analysis was performed by an unpaired *t*-test from 25 individual cells. **P* < 0.05, ***P* < 0.01, ****P* < 0.001.

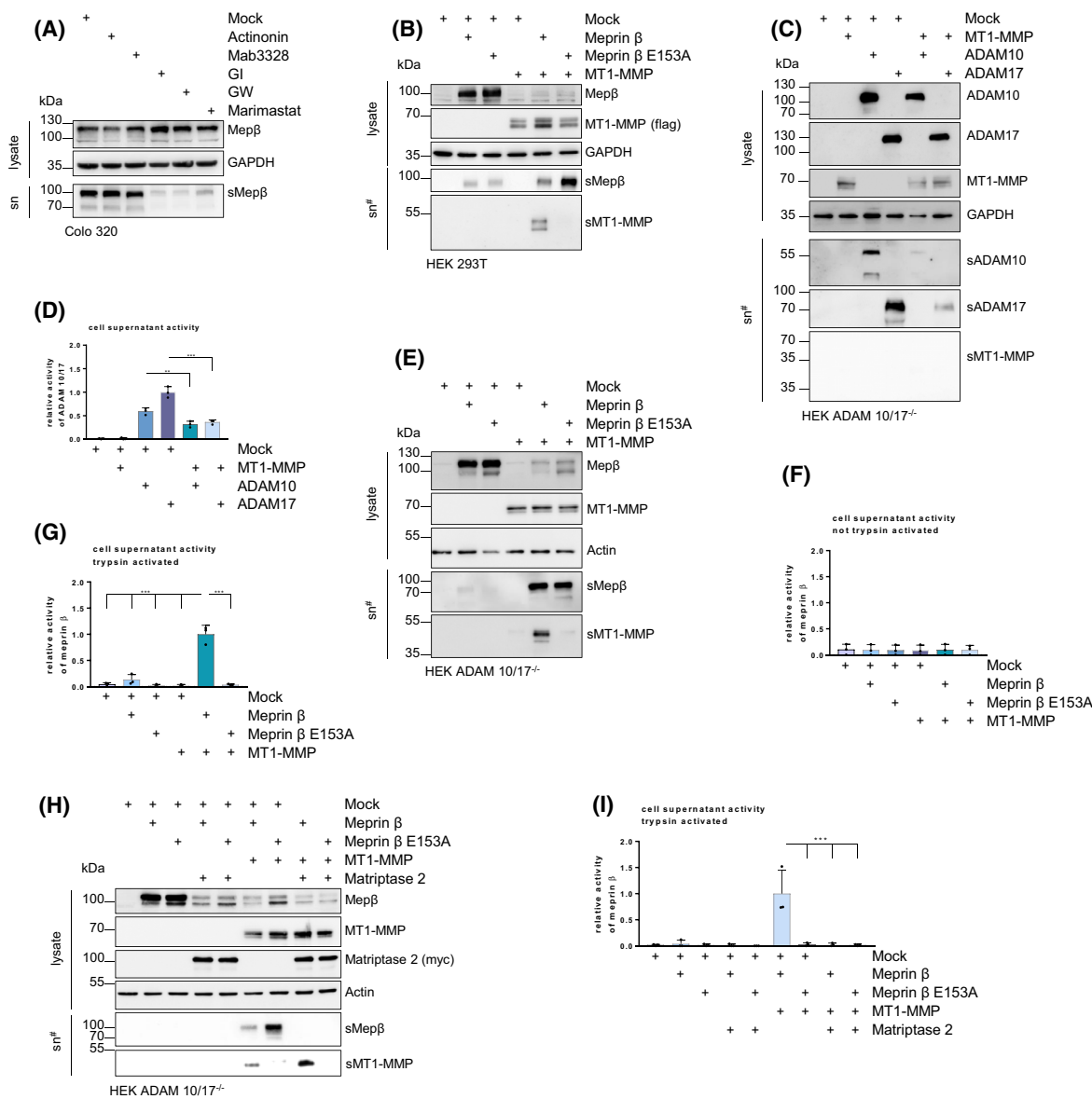


Fig. 3. Shedding of meprin β and MT1-MMP. (A) Colo 320 cells were treated with actinonin, Mab3328, GI, GW or marimastat. Immunoblotting was used to analyse cell lysates and supernatants. For detection, a specific antibody against meprin β was used. GAPDH served as loading control. (B) Transfection of HEK 293T cells with human meprin β , human MT1-MMP or inactive human meprin β E153A. Immunoblotting was used to analyse cell lysates and supernatants, human MT1-MMP was C-terminal flag-tagged. For detection, specific antibodies against flag, meprin β and MT1-MMP were used. GAPDH served as loading control. (C) Transfection of HEK ADAM10/17^{-/-} cells with human MT1-MMP, human ADAM10 or murine ADAM17. Immunoblotting was used to analyse cell lysates and supernatants. For detection, specific antibodies against MT1-MMP, ADAM10 or ADAM17 were used. GAPDH served as loading control. (D) ADAM10/17 activity assay of ultracentrifuged supernatants of C. (E) Transfection of HEK ADAM10/17^{-/-} cells with human meprin β , human MT1-MMP or inactive human meprin β E153A. Immunoblotting was used to analyse cell lysates and supernatants. For detection, specific antibodies against meprin β and MT1-MMP were used. Actin served as loading control. (F) Meprin β activity assay of ultracentrifuged supernatants of E. (G) Meprin β activity assay of ultracentrifuged and trypsin-activated supernatants of E. (H) Triple-transfection of HEK ADAM10/17^{-/-} cells with human meprin β , human MT1-MMP, inactive human meprin β E153A and human matriptase 2. Immunoblotting was used to analyse cell lysates and supernatants, human matriptase 2 was C-terminal myc-tagged. For detection, specific antibodies against myc, meprin β and MT1-MMP were used. Actin served as loading control. (I) Meprin β activity assay shows results for ultracentrifuged and trypsin-activated supernatants of H (B, C, E, H: # All supernatants were ultracentrifuged and TCA-precipitated). GI, GI 254023X; GW, GW 280264X; Mep, meprin; sn, supernatant. Data for activity assays represent means \pm SD, statistical analysis was performed by 1-way ANOVA, followed by Tukey's *post hoc* test from three biological replicates. * $P < 0.05$, ** $P < 0.01$, *** $P < 0.001$.

Consequently, to investigate whether the induction of shed meprin β was a direct effect of MT1-MMP and not due to an increased proteolytic activity of ADAM10/17 at the PM, we co-transfected MT1-MMP and meprin β in HEK ADAM10/17^{-/-} cells. Since we obtained soluble fragments for both meprin β and MT1-MMP, whenever both proteases were present, we could verify a direct mutual shedding of MT1-MMP and meprin β (Fig. 3E). However, without activation by trypsin, the shed meprin β fragment showed no proteolytic activity against a meprin β -specific fluorogenic substrate, suggesting that only inactive pro-meprin β is shed by MT1-MMP (Fig. 3F, G). This is in line with previous findings, as ADAM10/17 was only able to shed meprin β in its inactive pro-form [14], which could be verified herein by triple-transfection experiments in HEK ADAM10/17^{-/-} cells. Thus, following activation of meprin β on the PM via MT2, MT1-MMP was not able to cleave meprin β anymore, as demonstrated by immunoblotting and activity assays (Fig. 3H,I). Moreover, activation of meprin β by MT2 led to increased MT1-MMP shedding, as seen in the ultracentrifuged supernatant blot (Fig. 3H). In the following, we wanted to focus on the interaction between meprin β and MT1-MMP, therefore we decided to proceed with the HEK ADAM10/17^{-/-} cells.

Shedding of meprin β is a direct effect of MT1-MMP activity

To validate that the shedding of meprin β can be directly mediated by MT1-MMP, we used a catalytically inactive MT1-MMP variant (E240A-pH) [35] and investigated its shedding capacity towards meprin β *in vitro*. Importantly, the insertion of the pHluorin-tag between the hemopexin-like domain and the transmembrane domain did not influence the shedding capability of MT1-MMP with regard to meprin β , as seen in immunoblots and activity assays (MT1-MMP-pH, Fig. 4A,B). Strikingly, the use of inactive MT1-MMP E240A-pH resulted in the complete absence of shed meprin β (Fig. 4A,B). Furthermore, we used marimastat and the inhibitory antibody against the ectodomain of MT1-MMP (Mab3328) and analysed the cleavage of meprin β . The shedding capability of MT1-MMP towards meprin β was reduced by 50% using the antibody, whereas marimastat almost fully abolished the shedding of meprin β (Fig. 4C,D). The western blot results were validated by employing the meprin β -specific activity assay (Fig. 4E).

To further prove that the shedding of meprin β is a direct effect of MT1-MMP, we investigated the

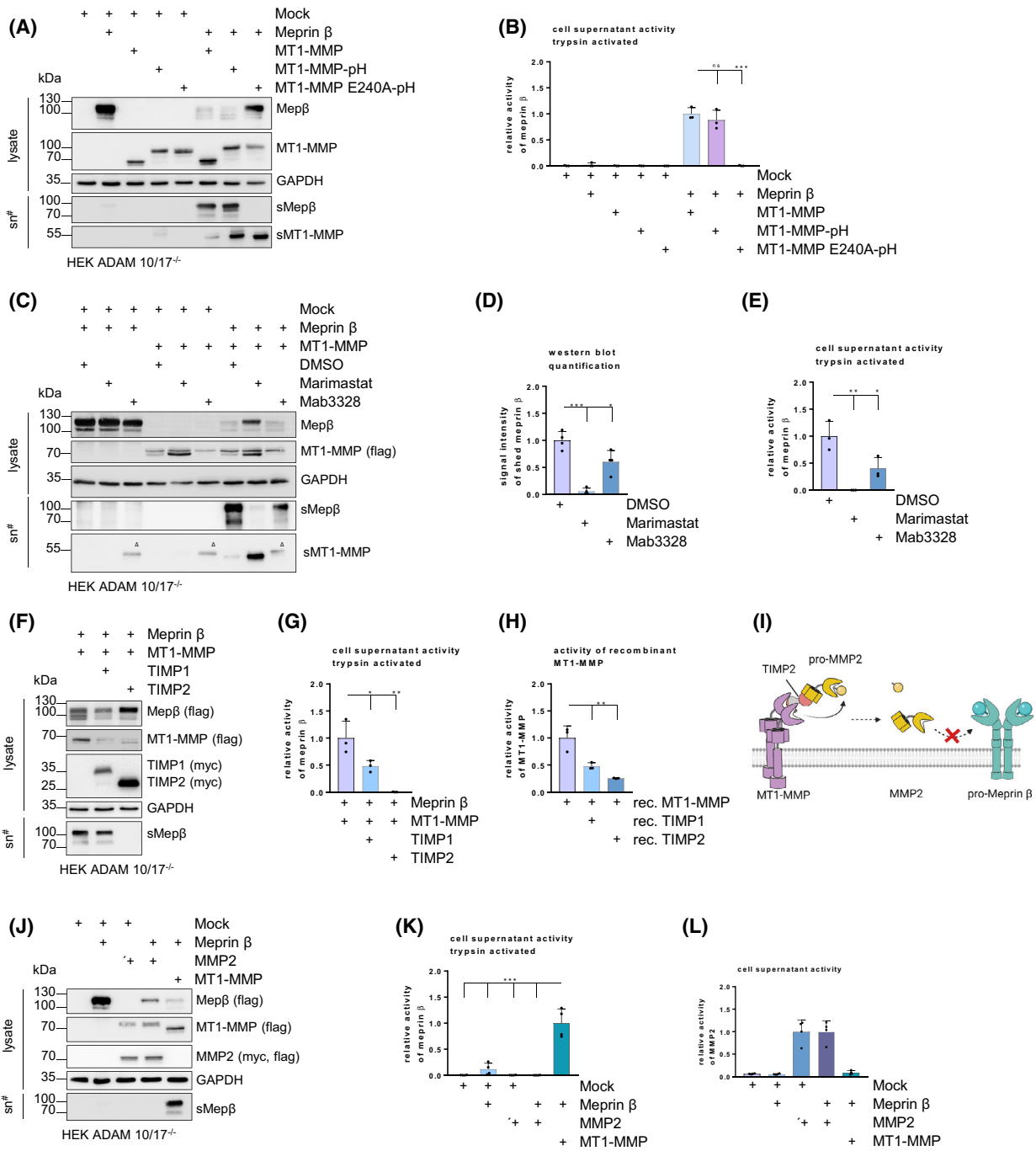
influence of tissue inhibitors of metalloproteinases (TIMP) 1 or TIMP2, when overexpressed in meprin β and MT1-MMP transfected HEK ADAM10/17^{-/-} cells. TIMP1 has been described to block most soluble MMPs but is a weak inhibitor for MT-MMPs, whereas TIMP2 inhibits all MMPs [36]. Immunoblot analysis revealed only a slight decrease in the shedding capability of MT1-MMP regarding meprin β when TIMP1 was co-expressed (Fig. 4F). In contrast, overexpression of TIMP2 led to a complete loss of shed meprin β , demonstrated by western blot and activity assay (Fig. 4F,G). Additionally, we tested the direct effect of recombinant TIMP1 or TIMP2 on recombinant MT1-MMP via an activity assay with an MT1-MMP-cleavable fluorogenic substrate. Indeed, the effects of recombinant TIMP1 and TIMP2 on recombinant MT1-MMP were similar to the results from the cell culture experiments (Fig. 4H).

Furthermore, we investigated if the shedding of meprin β is an effect of a subsequent downstream target of MT1-MMP. It has been described before that MT1-MMP together with TIMP2 is able to activate pro-MMP2 at the PM, leading to increased activity of MMP2 [16] (Fig. 4I). To exclude that MMP2 is the corresponding protease that cleaves meprin β , HEK ADAM10/17^{-/-} cells were transfected with MMP2 and meprin β . Here, no shedding of meprin β was detectable, indicating that activation of MMP2 by MT1-MMP is obviously not the reason for meprin β shedding (Fig. 4J,K). Of note, overexpression of MMP2 in HEK ADAM10/17^{-/-} cells also generates active protease, as validated by activity assays of the corresponding supernatants with an MMP2-cleavable fluorogenic substrate (Fig. 4L).

The mutual shedding of MT1-MMP and meprin β is restricted to human variants

The use of soluble recombinant MT1-MMP did not lead to any shed meprin β when added to meprin β transfected HEK ADAM10/17^{-/-} cells (Fig. 5A,B), which is in line with the previously described impaired shedding ability of soluble ADAM10/17 regarding meprin β [21]. Additionally, soluble and active recombinant meprin β did not induce MT1-MMP shedding either, as indicated by immunoblotting (Fig. 5C). Of note, shed meprin β is inactive (Fig. 3F,G) and therefore could not be the reason for shed MT1-MMP, when meprin β and MT1-MMP were co-expressed in HEK ADAM10/17^{-/-} cells (Fig. 5C).

Next, we were interested in whether the shedding of meprin β by MT1-MMP was species dependent. Thus, we transfected HEK ADAM10/17^{-/-} cells with the



human or murine variants of MT1-MMP and meprin β . Immunoblot analysis indicated that only human MT1-MMP was capable of shedding human meprin β from the PM, leading to a proteolytic active fragment upon trypsin activation (Fig. 5D–F). Similar results were investigated for the shedding of MT1-MMP, as only human meprin β was able to shed its human variant (Fig. 5D,E). To exclude possible interspecies

influences, we repeated the experiments in murine embryonal fibroblasts (MEF) which were deficient in ADAM10/17 (MEF ADAM10/17^{-/-}) and observed similar results (Fig. 5G). We speculated that the absence of shed murine meprin β *in vitro* could be due to differences in the cleavage region of murine and human meprin β . It has been described before that the replacement of the sequence of the putative ADAM17

Fig. 4. Shedding of meprin β is a direct effect of MT1-MMP. (A) Transfection of HEK ADAM10/17^{-/-} cells with human meprin β , human MT1-MMP, a pHluorin-tagged human variant of MT1-MMP (MT1-MMP-pH) or an inactive and pHluorin-tagged variant of human MT1-MMP (MT1-MMP E240A-pH). Immunoblotting was used to analyse cell lysates and supernatants. For detection, specific antibodies against MT1-MMP and meprin β were used. GAPDH served as loading control. (B) Meprin β activity assay of A shows results for ultracentrifuged and trypsin-activated supernatants. (C) Transfection of HEK ADAM10/17^{-/-} cells with human meprin β , human MT1-MMP and treatment with marimastat or Mab3328. Immunoblotting was used to analyse cell lysates and supernatants, MT1-MMP was C-terminal flag-tagged. For detection, specific antibodies against flag, MT1-MMP and meprin β were used. GAPDH served as loading control. (D) Quantitative western blot analysis of four individual experiments of C. (E) Meprin β activity assay of ultracentrifuged supernatants of C. (F) Transfection of HEK ADAM10/17^{-/-} cells with human meprin β , human MT1-MMP, human TIMP1 and human TIMP2. Immunoblotting was used to analyse cell lysates and supernatants, meprin β and MT1-MMP were C-terminal flag-tagged, TIMP1 and TIMP2 were C-terminal myc-tagged. For detection, specific antibodies against meprin β , flag and myc were used. GAPDH served as loading control. (G) Meprin β activity assay of F shows results for ultracentrifuged and trypsin-activated supernatants. (H) Activity assay of recombinant MT1-MMP in HEPES buffer shows the direct effect of recombinant TIMP1 and TIMP2 on its activity. (I) Schematic illustration of the activation of pro-MMP2. (J) Transfection of HEK ADAM10/17^{-/-} cells with human meprin β , human MMP2 or human MT1-MMP. Immunoblotting was used to analyse cell lysates and supernatants, human meprin β , human MT1-MMP and human MMP2 were C-terminal flag-tagged, human MMP2 was C-terminal myc-tagged. For detection, specific antibodies against flag, myc or meprin β were used. GAPDH served as loading control. (K) Meprin β activity assay of J shows results for ultracentrifuged and trypsin-activated supernatants. (L) MMP2 activity assay of ultracentrifuged supernatants of J (A, C, F, J: # All supernatants were ultracentrifuged and TCA-precipitated; C: ^A Unspecific signals of Mab3328). Mep, meprin; sn, supernatant; rec., recombinant. Data for activity assays represent means \pm SD, statistical analysis was performed by 1-way ANOVA, followed by Tukey's *post hoc* test from three (or four for K, L) biological replicates. * $P < 0.05$, ** $P < 0.01$, *** $P < 0.001$.

shedding region from human meprin β (₅₉₅QIQLT-PAPS₆₀₃) [37] to murine meprin β (₅₉₆SAVPDPVPTLA₆₀₆) inhibited the shedding of this cloned meprin β chimera (Fig. 5H) by ADAM10/17 *in vitro* [14]. As expected, shedding of the meprin β chimera by MT1-MMP was also completely inhibited, when both constructs were co-transfected in HEK ADAM10/17^{-/-} cells, verifying the particular importance of this amino acid sequence (Fig. 5I,J). Hence, MT1-MMP and ADAM10 could also use the same proposed cleavage region between Gln₅₉₅ and Ser₆₀₃.

The shedding of human meprin β occurs between Pro₆₀₂ and Ser₆₀₃

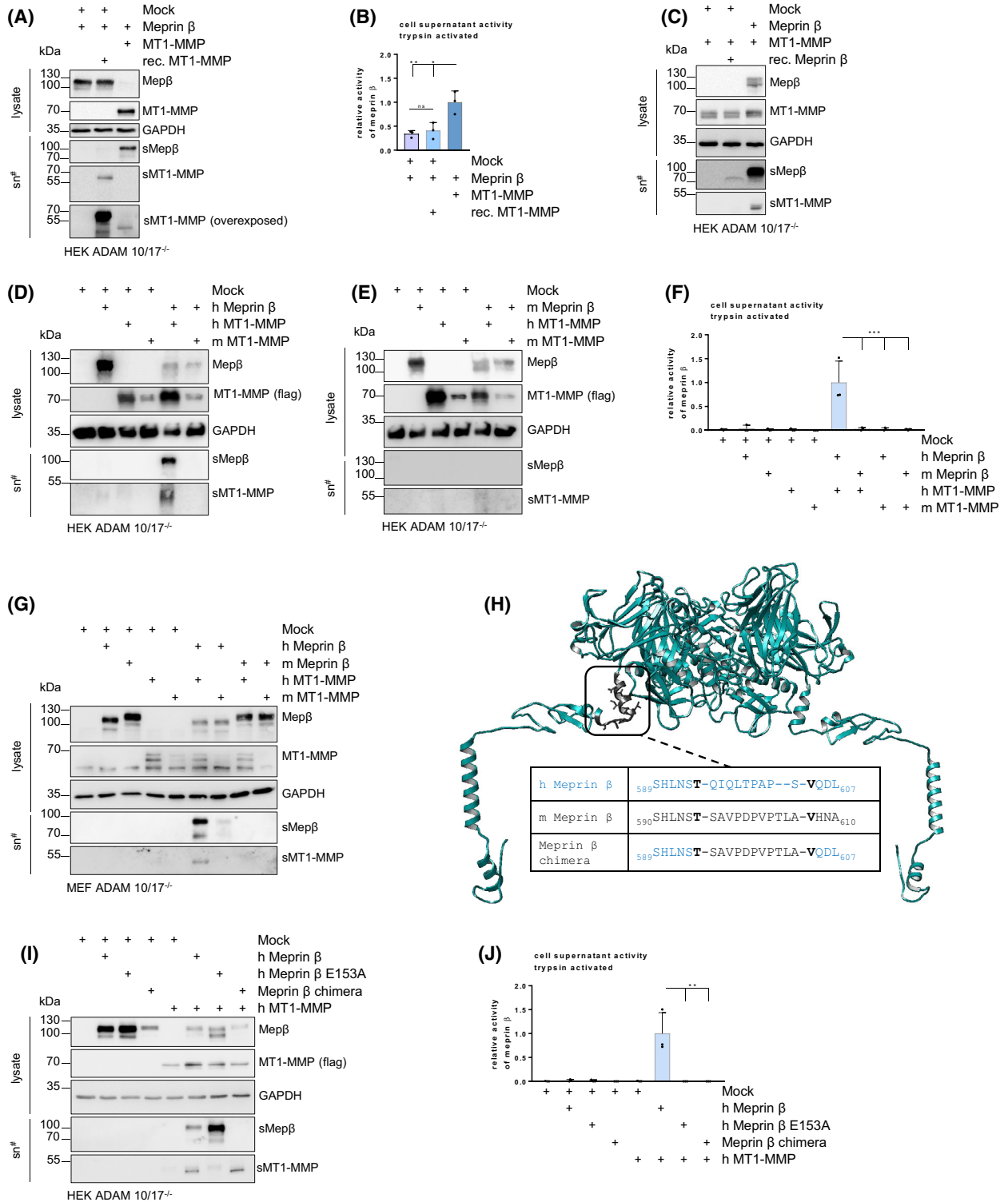
To identify the exact shedding site of meprin β used by its sheddases, we first transfected HEK ADAM10/17^{-/-} cells with MT1-MMP, ADAM10 or ADAM17 and human meprin β and compared the corresponding cleavage fragments. Immunoblot analysis revealed a similar size of the shed meprin β fragments generated by either MT1-MMP or ADAM10/17 (Fig. 6A). Next, we repeated the co-transfections in HEK ADAM10/17^{-/-} cells with MT1-MMP, ADAM10 or ADAM17 and human meprin β . Thereafter, Prot-G-Sepharose beads coupled with an antibody against the C-terminal part of meprin β were used to purify the remaining membrane-stubs from the lysate. Subsequently, samples underwent separation via SDS/PAGE and the meprin β C-terminal fragments were excised and analysed by liquid chromatography-mass spectrometry (LC/MS), to identify the cleavage sites. Surprisingly, the most abundant dimethylated peptides for meprin β

shedding by MT1-MMP, ADAM10 and ADAM17 revealed the identical cleavage site between Pro₆₀₂ and Ser₆₀₃ (Fig. 6B–D). Thus, cleavage of meprin β by all three sheddases indeed occurs in the expected region between Gln₅₉₅ and Ser₆₀₃.

Discussion

Herein, we could show that besides ADAM10/17, human MT1-MMP is able to shed human meprin β in co-transfection experiments in HEK 293T, HEK ADAM10/17^{-/-} and MEF ADAM10/17^{-/-} cells. Surprisingly, the cleavage site in meprin β used by all three sheddases is identical and located between Pro₆₀₂ and Ser₆₀₃.

Cleavage of meprin β by MT1-MMP is indeed a direct proteolytic event and not due to downstream-activated MMP2 [38]. Along the same line, MT1-MMP was described to activate pro-MMP13 at the PM, a process that is independent of TIMP2 [39]. However, TIMP1, described to block both MMP2 and MMP13 [36,40], did not prevent meprin β shedding, when co-transfected with meprin β and MT1-MMP, underlining the assumption that MT1-MMP is the (main) sheddase. The minor decrease of shed meprin β upon co-expression of TIMP1 can be explained by the mild effect of this inhibitor on the activity of MT1-MMP, as demonstrated herein. Moreover, RNAseq data revealed very low endogenous levels of MMP2 or MMP13 in HEK cells, demonstrating that direct shedding of meprin β by these proteases is even less likely [41]. Furthermore, we could show that meprin β itself is also able to cleave MT1-MMP, implicating a



complex regulatory network of these proteases in health and disease (Fig. 7). More interestingly, all observed shedding properties of MT1-MMP with

regard to meprin β appeared to be similar to its shedding by ADAM10/17 [14], including the same cleavage site between Pro₆₀₂ and Ser₆₀₃, which is in line with

Fig. 5. Specificity of the shedding of meprin β and MT1-MMP. (A) Transfection of HEK ADAM10/17^{-/-} cells with human meprin β and/or human MT1-MMP and treatment with recombinant active human MT1-MMP. Immunoblotting was used to analyse cell lysates and supernatants. For detection, specific antibodies against MT1-MMP and meprin β were used. GAPDH served as loading control. (B) Meprin β activity assay shows results for ultracentrifuged and trypsin-activated supernatants of A. (C) Transfection of HEK ADAM10/17^{-/-} cells with human meprin β and/or human MT1-MMP and treatment with recombinant active human meprin β . Immunoblotting was used to analyse cell lysates and supernatants. For detection, specific antibodies against MT1-MMP and meprin β were used. GAPDH served as loading control. (D, E) transfection of HEK ADAM10/17^{-/-} cells with human meprin β , murine meprin β , human MT1-MMP or murine MT1-MMP. Immunoblotting was used to analyse cell lysates and supernatants. Both, human MT1-MMP and murine MT1-MMP were C-terminal flag-tagged. For detection, specific antibodies against MT1-MMP, flag and meprin β were used. GAPDH served as loading control. (F) Meprin β activity assay shows results for ultracentrifuged and trypsin-activated supernatants of D and E. (G) transfection of MEF ADAM10/17^{-/-} cells with human meprin β , murine meprin β , human MT1-MMP or murine MT1-MMP. Immunoblotting was used to analyse cell lysates and supernatants. For detection, specific antibodies against MT1-MMP and meprin β were used. GAPDH served as loading control. (H) Schematic model of dimeric meprin β at the PM (based on the crystal structure of the ectodomain PDB: 4GWM), showing the sequence differences in the putative ADAM17 cleavage region between human (blue) and murine (black) meprin β . Figure was generated using CHIMERA 1.14. (I) Transfection of HEK ADAM10/17^{-/-} cells with human meprin β , human meprin β E153A, meprin β chimera or human MT1-MMP. Immunoblotting was used to analyse cell lysates and supernatants, human MT1-MMP was C-terminal flag-tagged. For detection, specific antibodies against MT1-MMP, flag and meprin β were used. GAPDH served as loading control. (J) Meprin β activity assay shows results for ultracentrifuged and trypsin-activated supernatants of I (A, C, D, E, G, I: # All supernatants were ultracentrifuged and TCA-precipitated). Mep, meprin; h, human; m, murine; rec., recombinant; sn, supernatant. Data for activity assays represent means \pm SD, statistical analysis was performed by 1-way ANOVA, followed by Tukey's *post hoc* test from three biological replicates. * $P < 0.05$, ** $P < 0.01$, *** $P < 0.001$.

the previously described common ADAM10/17 and MT1-MMP cleavage site specificity [42,43].

MT1-MMP is ubiquitously expressed in various cell types, including fibroblasts [44], epithelial cells [45], macrophages [35] or neuronal cells [46]. On the contrary, meprin β is more restricted to the small intestine [47], kidney [48] or the human epidermis [49]. Herein, we could show that MT1-MMP and meprin β also interact with each other endogenously. Nevertheless, the elucidation of the endogenous shedding between MT1-MMP and meprin β is difficult, as MT1-MMP also seems to interfere with the activity of ADAM10 and ADAM17. Thus, the use of a specific inhibitory antibody against MT1-MMP did not lead to a reduced shedding of meprin β in Colo 320 cells, possibly due to compensatory effects of ADAM10/17, which are widely expressed in almost all tissues. Actinonin has also been described to block the activity of ADAM10 (IC₅₀ of 2.2 μ M) and ADAM17 (IC₅₀ of 0.2 μ M) but not MT1-MMP (IC₅₀ > 1000 μ M) [50]. Hence, it is noteworthy that its use also did not prevent meprin β shedding in Colo 320 cells. GI254023X is generally described as a specific ADAM10 inhibitor (IC₅₀ of 0.027 μ M), however, it also affects the activity of MT1-MMP (IC₅₀ of 0.088 μ M) and ADAM17 (IC₅₀ of 0.86 μ M) [51]. A similar inhibitory effect with regard to MT1-MMP is also conceivable for GW208264X. Moreover, there are numerous interactions of all involved proteases with several other factors, which have to be considered. For instance, MT1-MMP is able to shed ADAM9 [52], which can cleave ADAM10 itself [21,53] and would consequently lead to altered shedding of meprin β [14]. Additionally, meprin β was

shown to cleave off the pro-peptides of ADAM9, -10 and -17, thereby inducing their activity [32]. Thus, it is hard to determine a direct effect of MT1-MMP on meprin β endogenously.

MT1-MMP knockout mice show severe defects during early development such as craniofacial abnormalities, dwarfism, arthritis and soft tissue fibrosis, which arise most likely due to altered collagen homeostasis [54]. However, meprin β knockout mice display significantly lower collagen deposition in the skin and exhibit a decreased tissue tensile strength [8]. Thus, investigation of these competitive proteolytic processes of MT1-MMP and meprin β , regarding collagen assembly *in vivo* would be interesting (Fig. 7). Unfortunately, our available meprin β mouse models were not suitable, as human MT1-MMP only cleaves human meprin β . Hence, the *in vivo* relevance of this proteolytic interaction remains elusive.

However, comparing the shedding region of human meprin β with other species, it is remarkable that they often contain additional possible O-glycosylation sites. It has been described before that O- and N-glycosylations can protect proteins from proteolysis [55,56]. For instance, shedding of tumour necrosis factor alpha (TNF- α) by ADAM17 was inhibited by site-specific O-glycosylation [56], while O-linked glycans within the cleavage region of human meprin β have also been described to protect from proteolysis [57]. A similar mechanism could also be a conceivable explanation for the difference in murine and human meprin β shedding. In particular, murine meprin β could additionally harbour an O-glycan at position Thr₆₀₄, protecting it from proteolysis. In general, glycosylation

Fig. 6. The shedding of meprin β by ADAM10/17 and MT1-MMP occurs between Pro₆₀₂ and Ser₆₀₃. (A) Transfection of HEK ADAM10/17^{-/-} cells with human meprin β , human MT1-MMP, human meprin β E153A, human ADAM10 or murine ADAM17. Immunoblotting was used to analyse cell lysates and supernatants, ADAM10 and MT1-MMP were C-terminal flag-tagged. For detection, specific antibodies against meprin β , flag, ADAM17 and MT1-MMP were used. Actin served as loading control. (B) Schematic model of dimeric meprin β at the PM (based on the crystal structure of the ectodomain PDB: 4GWM), illustrating the same cleavage site of ADAM10/17 and MT1-MMP in human meprin β . Figure was generated using CHIMERA 1.14. (C) A representative MS-spectrum of the meprin β peptide P.S603VQDLCSKTTCKNDGVCTVR.D that was identified following transfection of HEK ADAM10/17^{-/-} cells with MT1-MMP, ADAM10 and ADAM17 and subsequent in-gel reductive dimethylation and trypsin digestion. The peptide shown is carbamidomethylated on the cysteine residues, dimethylated at the lysine residue and dimethylated at the N-terminus. Monoisotopic m/z : 804.7282 ($z = 3$). (D) Dimethylated N-termini identified in MS-samples. N-termini which exhibit trypsin-like specificity (R residue at the P1 position) are likely a result of incomplete quenching prior to tryptic digestion.

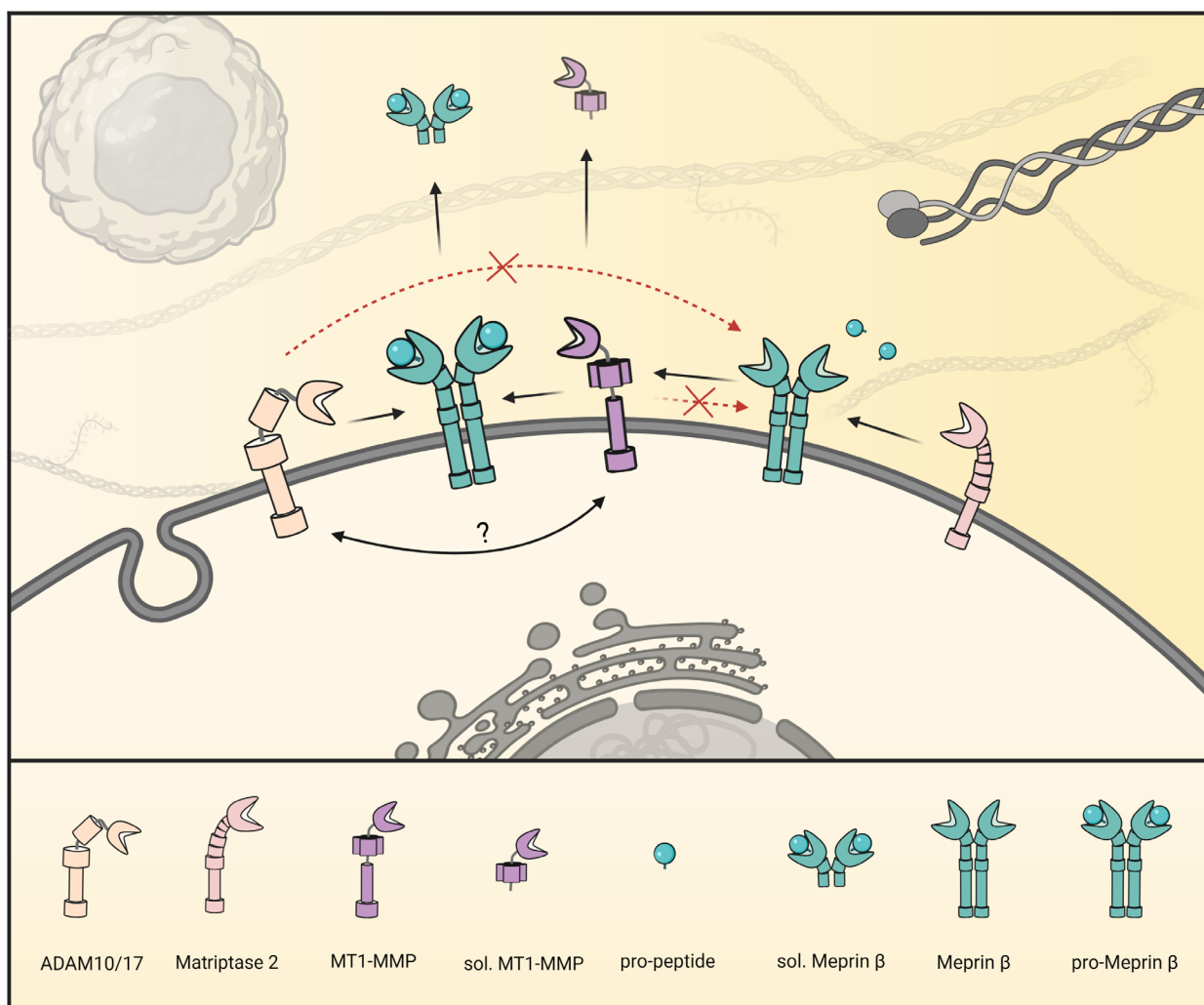


Fig. 7. Model of the interactions between meprin β , MT1-MMP and ADAM10/17 at the PM. ADAM10, ADAM17 and MT1-MMP are able to cleave pro-meprin β from the PM, leading to inactive soluble meprin β . Activation of meprin β on the PM via matriptase 2 completely abolishes its shedding by ADAM10/17 and MT1-MMP. Interestingly, human meprin β can also shed human MT1-MMP and both ADAM10 and ADAM17 seem to interact with MT1-MMP.

seems to be an important topic for meprin β , as the point mutations N592S and A601T within the shedding region of meprin β can be found in the COSMIC

database and are associated with endometrioid carcinoma and malignant melanoma, respectively [58]. Therefore, further studies regarding the glycosylation

status of meprin β could provide new insight into its regulation and could reveal new therapeutic options for the treatment of various pathological conditions.

Materials and methods

Chemicals

All chemicals were of analytical grade and received from Carl Roth (Karlsruhe, Germany), Gibco (Waltham, MA, USA), Merck (Darmstadt, Germany), Millipore-Sigma (Burlington, MA, USA) or Thermo Fisher Scientific (Waltham, MA, USA), if not stated otherwise.

Cell culture, transient transfection and inhibitor experiments

HEK 293T cells (DSMZ GmbH, Braunschweig, Germany), HEK ADAM10/17^{-/-} cells (kindly provided by Björn Rabe, University of Kiel, Germany), HeLa cells (DSMZ GmbH), MEF ADAM10/17^{-/-} cells (kindly provided by Karina Reiss, Department of Dermatology and Allergology, University Medical Center Schleswig-Holstein, Kiel, Germany), Colo 320 and Colo 320 MEP1B^{-/-} cells were cultivated in DMEM (Dulbecco's modified Eagle's medium, Gibco) with 10% (v/v) fetal calf serum (FCS, Gibco), 100 U·mL⁻¹ penicillin and 100 mg·mL⁻¹ streptomycin. Culture conditions were under a humidified atmosphere (5% CO₂) at 37 °C. For transient transfection, cells were seeded on 10-cm cell culture dishes or 6-well plates, 8 μ g (double-transfection) or 12 μ g (triple-transfection) of total cDNA were mixed with polyethylenimine (PEI) (HEK cells) or Turbofect (MEF cells) transfection reagent (1:3) in serum-free medium and incubated for 30 min at room temperature (RT). For transfection, plasmid-cDNA for human meprin β , human meprin β E153A, human MT1-MMP, human MT2, murine MT1-MMP, murine meprin β , human ADAM10, murine ADAM17, meprin β chimera (kindly provided by Rielana Wichert, University of Kiel, Germany), human MT1-MMP-pHluorin (kindly provided by Philippe Chavrier, Institut Curie, Paris, France), human MT1-MMP E240A-pHluorin, human TIMP1, human TIMP2, human MMP2, human APP695, human IL-6R, empty vector (pcDNA 3.1) or plasmids in various combinations were added together with the transfection reagent to 3 mL (10 cm dish) or 1.5 mL (6-well plate) fresh medium on the cells. After 6 h, cells were washed with PBS and maintained in serum-free DMEM to avoid meprin β inhibition [59]. For the inhibitor experiments in HEK ADAM10/17^{-/-} cells, marimastat (10 μ M) or Mab3328 (10 μ g·mL⁻¹, Merck) were added. For endogenous inhibition in Colo 320 cells, actinonin (3 μ M), Mab3328 (10 μ g·mL⁻¹), GI254023X (3 μ M, Millipore-Sigma), GW208264X (3 μ M, AOBIOUS, Gloucester, MA, USA) or marimastat (3 μ M) were used. Recombinant human meprin β [60] was used in a

concentration of 5 nM and recombinant human MT1-MMP (918-MPN-010, R&D Systems, Minneapolis, MN, USA) was used 0.05 μ g·mL⁻¹. Cells were harvested 24 h after media was exchanged.

Generation of meprin β -deficient Colo 320 cell line using CRISPR/Cas9 genome editing

Colo 320 cells were cultivated in DMEM supplemented with 10% FCS. For CRISPR/Cas9 genome editing multi-guide RNA (G*U*C*UUCAGUAGGAAAUAGGC, C*A*A*GAGUCCUCCACGCUCU, U*U*A*UCCUGACAUAGUCAUCC) and recombinant *Streptococcus pyogenes* Cas9 2NLS (Synthego, Redwood City, CA, USA) were used. Cas9 RNPs were prepared according to Synthego's instructions with 100 pmol multi-guide RNA and 20 pmol Cas9 per electroporation using 7.6×10^4 cells and the Neon device (Thermo Fisher Scientific) with the following setting: 1 puls, 1700 V, 20 ms. Immediately after electroporation, single cell seeding in 96-well plates was performed to obtain single-cell clones. From these, genomic DNA was extracted using the GeneJET Genomic DNA Purification Kit (Thermo Fisher Scientific) and genotyping PCRs with the following primers were performed: for: 5'-GACTAGGCAGTGGCGATTCTG-3', rev: 5'-CCACAGACTCCGTTCCACATA-3'.

Cell lysis, SDS/PAGE and immunoblot analysis

Cells were harvested 30 h after transfection in ice-cold PBS and centrifuged at 1100 *g* for 10 min at 4 °C. The remaining cell pellets were washed 3 \times with PBS prior to resuspension in lysis buffer [1% (v/v) Triton X-100, complete protease inhibitor cocktail (Roche, Basel, Switzerland) in PBS, pH 7.4], following a 60 min incubation on ice. Afterwards, cell suspensions were centrifuged for 15 min at 15 000 *g* and 4 °C. The protein amount was determined using the Bicinchoninic Acid Protein Assay Kit (Thermo Fisher Scientific). The remaining lysates were boiled for 10 min at 95 °C in sample buffer containing dithiothreitol (DTT). Supernatants were also harvested 30 h after transfection and ultracentrifuged at 186 000 *g* for 120 min at 4 °C. Afterwards, 10% (v/v) trichloroacetic acid (TCA) was added and samples were incubated 60 min on ice, before centrifugation at 15 000 *g* and 4 °C for 15 min. Supernatants were discarded, 200 μ L ice-cold acetone was added and samples were again centrifuged at 15 000 *g* and 4 °C for 10 min. Subsequently, a sample buffer containing DTT was added and samples were boiled for 10 min at 95 °C. For further analysis, protein samples were separated via SDS/PAGE (10%, 120 V, 100 min), blotted onto a polyvinylidene fluoride (PVDF, Thermo Fisher Scientific) membrane and incubated with 10% dry milk for 1 h at RT. Afterwards, the membranes were incubated with primary antibody (1:1000 in 5% dry milk)

overnight at 4 °C. The next day, membranes were washed with TRIS-buffered saline (TBS) and secondary antibodies (1:20 000 in 5% dry milk) conjugated with horseradish peroxidase were added. After 1 h incubation at RT, membranes were washed with TBS and chemiluminescence was detected using the SuperSignal West Femto Kit (Thermo Fisher Scientific) and the LAS-3000 Imaging System (FUJIFILM Europe GmbH). For detection, the following antibodies were used: anti-meprin β Tier 1 (polyclonal, generated against the peptide ₂₇₃CGMIQSSGDSADWQRVSQ₂₉₀, Pineda, Berlin, Germany); anti-flag (F1804, Millipore-Sigma); anti-actin (A2066, Millipore-Sigma); anti-MT1-MMP (inhibitory antibody against the ectodomain, Mab3328, also known as LEM-2/15, Merck); anti-MT1-MMP (#51074, Abcam); anti-myc (#2276, Cell-Signalling); anti-GAPDH (#2118, Cell-Signalling); anti-ADAM17 (#19027, Merck); anti-IL-6R (4–11, monoclonal, generated against the D1-domain); anti-APP (CT-15, AG Pietrzik, Mainz); anti-APP (22C11, Thermo Fisher Scientific); anti-sAPP β (generated against the neo-C-terminus of sAPP β between Asp₆₇₂ and Ala₆₇₃, that is released after APP shedding by meprin β); anti-mouse IgG (H + L)-HRP (Jackson Immuno Research, Ely, UK); anti-rabbit IgG (H + L)-HRP (Jackson Immuno Research).

Immunofluorescence microscopy

HeLa cells were seeded into 24-well plates containing small cover slips and were transfected with 1 μ g plasmid-cDNA of MT1-MMP-pH and flag-tagged meprin β using PEI. After 24 h, cells were washed 3 \times with PBS and were fixed in 4% (w/v) paraformaldehyde (PFA) in PBS for 10 min at RT. Subsequently, cells were washed 2 \times with PBS and were permeabilized with 0.12% (w/v) glycine and 0.2% (w/v) saponin in PBS for 10 min and RT. Thereafter, cells were treated with blocking solution [10% FCS, 0.2% (w/v) saponin in PBS] for 1 h at RT, prior to incubation of the coverslips with 60 μ L anti-flag antibody solution (F1804, Millipore-Sigma, 1:1000 in blocking solution) in a humid chamber for 1 h and RT. Coverslips were washed 5 \times in 0.2% (w/v) saponin/PBS and incubated with 60 μ L of the fluorophore coupled secondary antibody (AlexaFluor-594 goat-anti-mouse IgG (H + L), Invitrogen, 1:300 in blocking solution) and DAPI (Roth, 1:1000 in blocking solution) for 1 h in a dark chamber. After 7 \times washing steps with 0.2% (w/v) saponin/PBS and ddH₂O, coverslips were mounted using 10 μ L Dako (S3023, Agilent, Santa Clara, CA, USA). Immunofluorescence analysis was performed using the confocal microscope FV1000 (Olympus, Tokyo, Japan).

Biotinylation

HEK ADAM10/17^{-/-} cells were cooled 30 h after transfection to 4 °C and supernatants were discarded. Cells were washed 2 \times with PBS-CM (0.1 mM CaCl₂, 1 mM MgCl₂, in

PBS, pH 7.4) and incubated with 3 mL Sulfo-NHS-SS-biotin solution (1 mg·mL⁻¹ in PBS-CM, Thermo Fisher Scientific) for 30 min at 4 °C. Next, cells were incubated with 10 mL quenching buffer (50 mM TRIS-HCl, in PBS-CM, pH 8.0) for 10 min at 4 °C, before cells were washed 3 \times with PBS-CM. Thereafter, cells were harvested in 1 mL PBS-CM, centrifuged for 10 min and 5000 *g* at 4 °C and lysed with 300 μ L lysis buffer [50 mM TRIS-HCl, 150 mM NaCl, 1% (v/v) Triton X-100, 0.1% (w/v) SDS, complete protease inhibitor cocktail + EDTA, pH 7.4] for 30 min at 4 °C. After centrifugation for 15 min and 15 000 *g* at 4 °C, 100 μ g of the supernatants were separated as lysate controls for immunoblot analysis. Subsequently, 500 μ g lysates were incubated with 50 μ L streptavidin magnetic beads (Thermo Fisher Scientific) for 1 h at 4 °C, before beads were washed 2 \times with lysis buffer. After discarding the supernatants, beads were boiled for 10 min at 95 °C in 35 μ L 1 \times Laemmli buffer containing DTT. Finally, samples were separated via SDS/PAGE and analysed by immunoblotting.

Immunoprecipitation

HEK ADAM10/17^{-/-} cells were transfected with human meprin β and human MT1-MMP (Co-IP, N-terminomics) or meprin β with ADAM10/17 (N-terminomics) and harvested as described above, cell pellets were lysed in 500 μ L lysis buffer (120 mM NaCl, 50 mM TRIS/HCl, 1% NP-40, complete protease inhibitor cocktail, pH 7.4). For lysis control, 50 μ L lysate was collected, and the remaining cell lysates were incubated with 1.5 μ L antibody [Co-IP: anti-meprin β Tier 1 or anti-MT1-MMP, #51074, Abcam; N-terminomics: meprin β C-terminal Tier 1 (polyclonal, generated against the peptide ₆₈₂CRERMSSNRPNLTPQNQHAF₇₀₁, Pineda)] at 4 °C overnight. The next day, 50 μ L Dynabeads (Thermo Fisher Scientific) were added to each vial and incubated for 30 min at RT. Thereafter, the tubes were placed on a magnet and were washed 3 \times with washing buffer (cf. manufacturer's instructions). At the end, beads were boiled for 10 min at 95 °C in sample buffer containing DTT and separated via SDS/PAGE. Subsequently, Co-IP was analysed by Immunoblot.

Proximity ligation assay

Colo 320 wild-type and meprin β -deficient Colo 320 cells were analysed using the Duolink *In Situ* Red Kit Mouse/Rabbit (Sigma-Aldrich). Cells were washed 3 \times with PBS and fixed in 4% (w/v) PFA in PBS for 10 min at RT. Subsequently, cells were washed 2 \times with PBS. For the C-terminal antibodies, cells were additionally permeabilized with 0.12% (w/v) glycine and 0.2% (w/v) saponin in PBS for 10 min. Thereafter, proximity ligation assay was performed according to the manufacturer's instructions using

the primary antibodies anti-meprin β C-term. Tier 2 (1:1000, Pineda) and anti-MT1-MMP C-term. (1:1000, sc-373908, Santa Cruz) or anti-meprin β hecto Serum Tier 1 (1:1000, binds to the ectodomain of meprin β , Pineda) and anti-MT1-MMP ecto. (1:1000, against the ectodomain, Mab3328, Merck). Immunofluorescence analysis was performed using the confocal laser scanning microscope LSM 980 (Carl Zeiss).

Fluorogenic peptide-based activity assay

To investigate the activity of meprin β , ADAM10/17, MMP2 or MT1-MMP, fluorogenic peptide-based activity assays were performed. Meprin β activity was measured using the substrate (mca)-EDEDED-(dnp) [61], ADAM10 and ADAM17 activity was measured using the substrate Dabcyl-PRAAAHomopheTSPK(5FAM)-NH₂ (PEPDAB064, BioZyme, Hessisch Oldendorf, Germany), MT1-MMP and MMP2 activity was analysed with the substrate Dabcyl-GPLGMRGK(5FAM)-NH₂ (PEPDAB011, BioZyme). For activity measurements of shed meprin β , shed ADAM10/17 or soluble MMP2, adjusted amounts of ultracentrifuged (186 000 g, 120 min, 4 °C) supernatants were filled into 96-well plates. For meprin β activity, supernatants were additionally incubated with 10 μ g recombinant trypsin (Sigma-Aldrich) or PBS as control for 30 min at 37 °C. MT1-MMP activity was measured by filling 90 μ L HEPES buffer, together with 0.05 μ g recombinant and active MT1-MMP and 0.5 μ g·mL⁻¹ recombinant TIMP1 or TIMP2 (#410-01, #410-02, PeproTech, Hamburg, Germany) into 96-well plates. Subsequently, 50 μ M (meprin β) or 10 μ M (ADAM10/17, MT1-MMP, MMP2) fluorogenic substrate was added and fluorescence was measured at λ_{em} = 405 nm and λ_{ex} = 320 nm (meprin β) or at λ_{em} = 530 nm and λ_{ex} = 485 nm (ADAM10/17, MT1-MMP, MMP2) at 37 °C every 30 s over a period of 2 h with a spectrophotometer (Infinite F200Pro, Tecan, Mannedorf, Switzerland). For bar graph presentation of data, the relative fluorescence units (RFU) after 40 min were used. The increase in RFU was normalized to the initial point of measurement and was proportional to meprin β , ADAM10/17, MT1-MMP or MMP2 activity.

Identification of protein N-termini

In-gel N-termini analysis

To identify the N-termini of the C-terminal meprin β fragments, the corresponding gel bands were excised, cut into 2 mm³ and destained with 100 mM ammonium bicarbonate (ABC), 30% acetonitrile (ACN), 50 mM ABC and 100% ACN. Immunoblots served as a template for excising the correct size of the C-terminal meprin β stubs from the SDS-gels. Samples were reduced with DTT (10 mM) at 65 °C for 30 min and then alkylated with iodoacetamide

(55 mM final) in the dark at RT for 15 min. Gel bands were washed with HEPES (100 mM), HEPES in ACN and ACN to remove any residual ABC buffer. Primary amines (N-termini and lysine residues) were reductively dimethylated by labelling with 20 mM formaldehyde in the presence of 10 mM sodium cyanoborohydride (10 mM) in HEPES buffer (100 mM, pH 7) overnight at 37 °C. The excess reagents were quenched by removing the supernatant and incubating the samples with 500 mM ABC (30 min), followed by 500 mM TRIS (pH 6.8). Samples were dehydrated with the addition of ACN (x2, 10 min) and then dried by vacuum centrifugation. Samples were again incubated with 0.5 M TRIS (pH 6.8) for 1 h. Gel bands were washed by incubating the gel pieces with ABC and ABC in ACN (30%) and 100% ACN, respectively. Gel bands were dried before trypsin (150 ng) was added to the gel pieces and left to incubate overnight at 37 °C. Peptides were extracted from the gel band using 1% formic acid (FA), 50% ACN, 1% FA and 100% ACN with the aid of sonication, respectively. Pooled supernatants were dried down by vacuum centrifugation and stored at -20 °C until analysis.

LC/MS measurements

Samples were injected on a Dionex Ultimate 3000 nano-UHPLC coupled to a Q Exactive Plus mass spectrometer (Thermo Scientific, Bremen, Germany). The samples were washed on a trap column (Acclaim Pepmap 100 C-18, 5 mm \times 300 μ m, 5 μ m, 100 Å, Dionex) for 2–3 min with 3% ACN/0.1% TFA at a flow rate of 30 μ L·min⁻¹ prior to peptide separation using an Acclaim PepMap 100 C-18 analytical column (50 cm \times 75 μ m, 2 μ m, 100 Å, Dionex). A flow rate of 300 nL·min⁻¹ using eluent A (0.05% FA) and eluent B (80% ACN/0.04% FA) was used for gradient separation (60 min gradient, 5–40% B). Spray voltage applied on a metal-coated PicoTip emitter (10 μ m tip size, New Objective, Woburn, MA, USA) was 1.6–1.8 kV, with a source temperature of 250 °C. Full scan MS-spectra were acquired between 300 and 2000 m/z at a resolution of 70 000 at m/z 400. The 10 most intense precursors with charge states greater than 2+ were selected with an isolation window of 1.6–2.1 m/z and fragmented by HCD with normalized collision energies of 27 at a resolution of 17 500. Lock mass (445.120025 m/z) and dynamic exclusion (15–20 s) were enabled.

Database search and statistics

The MS raw files were processed by PROTEOME DISCOVERER 2.2 (Thermo, version 2.2.0.388) and MS/MS spectra were searched using the Sequest HT algorithm against a database containing common contaminants and the canonical and reviewed human database. Enzyme specificity was set to semi-ArgC with two missed cleavages allowed. A MS1 tolerance of 10 ppm and a MS2 tolerance of 0.02 Da were implemented. Oxidation

(15.995 Da) of methionine residues was set as a variable modification while carbamidomethylation (57.02146 Da) on cysteine residues and dimethylation (28.031 Da) on lysine residues were set as static modifications. In addition, dimethylation on peptide N-termini was set as a variable modification. Minimal peptide length was set to 6 amino acids and the peptide false discovery rate was set to 1%.

Statistical analysis

Immunoblots were quantified with IMAGEJ (National Institutes of Health, Bethesda, MD, USA) and the proteins of interest were normalized to GAPDH levels. All statistical analyses were performed with GRAPHPAD PRISM (La Jolla, CA, USA) by 1-way ANOVA, followed by Tukey's *post hoc* test or by an unpaired student's *t*-test. Normalized values were presented as means \pm SD.

Acknowledgements

This work was supported by Deutsche Forschungsgemeinschaft (DFG) grants [SFB 877, Proteolysis as a Regulatory Event in Pathophysiology, Projects A9 (CB-P), B13 (SL) Z2 (TK, AT)] and SCHA 2248/2-1 (FS). Figures were created by LW, generated with Biorender.com. Open Access funding enabled and organized by Projekt DEAL.

Conflict of interest

The authors declare no conflict of interest. The funders had no role in the design of the study; in the collection, analyses, or interpretation of data; in the writing of the manuscript, or in the decision to publish the results.

Author contributions

Investigation and data analysis: LW, AG, KB, CB, FA, KP, MS, FS; N-terminomics was performed by TK; Resources: FS, KP, AT, SL; LW and CB-P drafted and edited the manuscript.

Peer review

The peer review history for this article is available at <https://publons.com/publon/10.1111/febs.16586>.

Data availability statement

The mass spectrometry-based proteomics data have been uploaded to the ProteomeXchange Consortium via the PRIDE [62] partner repository with the dataset identifier PXD032198.

References

- Minder P, Bayha E, Becker-Pauly C, Sterchi EE. Meprin α transactivates the epidermal growth factor receptor (EGFR) via ligand shedding, thereby enhancing colorectal cancer cell proliferation and migration. *J Biol Chem*. 2012;**287**:35201–11.
- Schönherr C, Bien J, Isbert S, Wichert R, Prox J, Altmeppen H, et al. Generation of aggregation prone N-terminally truncated amyloid β peptides by meprin β depends on the sequence specificity at the cleavage site. *Mol Neurodegener*. 2016;**11**:19.
- Biasin V, Wygrecka M, Marsh LM, Becker-Pauly C, Brcic L, Ghanim B, et al. Meprin beta contributes to collagen deposition in lung fibrosis. *Sci Rep*. 2017;**7**:39969.
- Arnold P, Boll I, Rothaug M, Schumacher N, Schmidt F, Wichert R, et al. Meprin metalloproteases generate biologically active soluble Interleukin-6 receptor to induce trans-signaling. *Sci Rep*. 2017;**7**:44053.
- Walker PD, Kaushal GP, Shah SV. Meprin a, the major matrix degrading enzyme in renal tubules, produces a novel nidogen fragment in vitro and in vivo. *Kidney Int*. 1998;**53**:1673–80.
- Werny L, Colmorgen C, Becker-Pauly C. Regulation of meprin metalloproteases in mucosal homeostasis. *Biochim Biophys Acta Mol Cell Res*. 2022;**1869**:119158.
- Peters F, Rahn S, Mengel M, Scharfenberg F, Otte A, Koudelka T, et al. Syndecan-1 shedding by meprin beta impairs keratinocyte adhesion and differentiation in hyperkeratosis. *Matrix Biol*. 2021;**102**:37–69.
- Broder C, Arnold P, Vadon-Le Goff S, Konerding MA, Bahr K, Muller S, et al. Metalloproteases meprin alpha and meprin beta are C- and N-procollagen proteinases important for collagen assembly and tensile strength. *Proc Natl Acad Sci USA*. 2013;**110**:14219–24.
- Kronenberg D, Bruns BC, Moali C, Vadon-Le Goff S, Sterchi EE, Traupe H, et al. Processing of procollagen III by meprins: new players in extracellular matrix assembly? *J Invest Dermatol*. 2010;**130**:2727–35.
- Kruppa D, Peters F, Bornert O, Maler MD, Martin SF, Becker-Pauly C, et al. Distinct contributions of meprins to skin regeneration after injury – Meprin alpha a physiological processor of pro-collagen VII. *Matrix Biol Plus*. 2021;**11**:100065.
- Grunberg J, Dumermuth E, Eldering JA, Sterchi EE. Expression of the alpha subunit of PABA peptide hydrolase (EC 3.4.24.18) in MDCK cells. Synthesis and secretion of an enzymatically inactive homodimer. *FEBS Lett*. 1993;**335**:376–9.
- Ohler A, Debela M, Wagner S, Magdolen V, Becker-Pauly C. Analyzing the protease web in skin: meprin metalloproteases are activated specifically by KLK4, 5 and 8 vice versa leading to processing of proKLK7 thereby triggering its activation. *Biol Chem*. 2010;**391**:455–60.

- 13 Jackle F, Schmidt F, Wichert R, Arnold P, Prox J, Mangold M, et al. Metalloprotease meprin beta is activated by transmembrane serine protease matriptase-2 at the cell surface thereby enhancing APP shedding. *Biochem J*. 2015;**470**:91–103.
- 14 Wichert R, Ermund A, Schmidt S, Schweinlin M, Ksiazek M, Arnold P, et al. Mucus detachment by host metalloprotease Meprin beta requires shedding of its inactive pro-form, which is abrogated by the pathogenic protease RgpB. *Cell Rep*. 2017;**21**:2090–103.
- 15 Nagase H. Activation mechanisms of matrix metalloproteinases. *Biol Chem*. 1997;**378**:151–60.
- 16 Itoh Y. Membrane-type matrix metalloproteinases: their functions and regulations. *Matrix Biol*. 2015;**44–46**:207–23.
- 17 Ohuchi E, Imai K, Fujii Y, Sato H, Seiki M, Okada Y. Membrane type 1 matrix metalloproteinase digests interstitial collagens and other extracellular matrix macromolecules. *J Biol Chem*. 1997;**272**:2446–51.
- 18 Okada Y, Morodomi T, Enghild JJ, Suzuki K, Yasui A, Nakanishi I, et al. Matrix metalloproteinase 2 from human rheumatoid synovial fibroblasts. Purification and activation of the precursor and enzymic properties. *Eur J Biochem*. 1990;**194**:721–30.
- 19 Weber S, Saftig P. Ectodomain shedding and ADAMs in development. *Development*. 2012;**139**:3693–709.
- 20 Kruse MN, Becker C, Lottaz D, Kohler D, Yiallourous I, Krell HW, et al. Human meprin alpha and beta homo-oligomers: cleavage of basement membrane proteins and sensitivity to metalloprotease inhibitors. *Biochem J*. 2004;**378**:383–9.
- 21 Scharfenberg F, Helbig A, Sammel M, Benzel J, Schlomann U, Peters F, et al. Degradome of soluble ADAM10 and ADAM17 metalloproteases. *Cell Mol Life Sci*. 2020;**77**:331–50.
- 22 Riethmueller S, Somasundaram P, Ehlers JC, Hung CW, Flynn CM, Lokau J, et al. Proteolytic origin of the soluble human IL-6R in vivo and a decisive role of N-glycosylation. *PLoS Biol*. 2017;**15**:e2000080.
- 23 Sammel M, Peters F, Lokau J, Scharfenberg F, Werny L, Linder S, et al. Differences in shedding of the interleukin-11 receptor by the proteases ADAM9, ADAM10, ADAM17, meprin α , meprin β and MT1-MMP. *Int J Mol Sci*. 2019;**20**:3677.
- 24 Bien J, Jefferson T, Causevic M, Jumpertz T, Munter L, Multhaup G, et al. The metalloprotease meprin beta generates amino terminal-truncated amyloid beta peptide species. *J Biol Chem*. 2012;**287**:33304–13.
- 25 Jefferson, T., Causevic, M., auf dem Keller, U., Schilling, O., Isbert, S., Geyer, R., Maier, W., Tschickardt, S., Jumpertz, T., Weggen, S., Bond, J. S., Overall, C. M., Pietrzik, C. U. & Becker-Pauly, C. (2011) Metalloprotease meprin beta generates nontoxic N-terminal amyloid precursor protein fragments in vivo, *J Biol Chem* **286**, 27741–50.
- 26 Higashi S, Miyazaki K. Novel processing of beta-amyloid precursor protein catalyzed by membrane type 1 matrix metalloproteinase releases a fragment lacking the inhibitor domain against gelatinase a. *Biochemistry*. 2003;**42**:6514–26.
- 27 Liao MC, Van Nostrand WE. Degradation of soluble and fibrillar amyloid beta-protein by matrix metalloproteinase (MT1-MMP) in vitro. *Biochemistry*. 2010;**49**:1127–36.
- 28 Garcia-Gonzalez L, Pilat D, Baranger K, Rivera S. Emerging alternative proteinases in APP metabolism and Alzheimer's disease pathogenesis: a focus on MT1-MMP and MT5-MMP. *Front Aging Neurosci*. 2019;**11**:244.
- 29 Asai M, Hattori C, Szabo B, Sasagawa N, Maruyama K, Tanuma S, et al. Putative function of ADAM9, ADAM10, and ADAM17 as APP alpha-secretase. *Biochem Biophys Res Commun*. 2003;**301**:231–5.
- 30 Becker-Pauly C, Pietrzik CU. The metalloprotease Meprin beta is an alternative beta-secretase of APP. *Front Mol Neurosci*. 2016;**9**:159.
- 31 Paumier JM, Py NA, Garcia-Gonzalez L, Bernard A, Stephan D, Louis L, et al. Proamyloidogenic effects of membrane type 1 matrix metalloproteinase involve MMP-2 and BACE-1 activities, and the modulation of APP trafficking. *FASEB J*. 2019;**33**:2910–27.
- 32 Wichert R, Scharfenberg F, Colmorgen C, Koudelka T, Schwarz J, Wetzel S, et al. Meprin beta induces activities of a disintegrin and metalloproteinases 9, 10, and 17 by specific prodomain cleavage. *FASEB J*. 2019;**33**:11925–40.
- 33 Miesenbock G. Synapto-pHluorins: genetically encoded reporters of synaptic transmission. *Cold Spring Harb Protoc*. 2012;**2012**:213–7.
- 34 Monteiro P, Rosse C, Castro-Castro A, Irondelle M, Lagoutte E, Paul-Gilloteaux P, et al. Endosomal WASH and exocyst complexes control exocytosis of MT1-MMP at invadopodia. *J Cell Biol*. 2013;**203**:1063–79.
- 35 El Azzouzi K, Wiesner C, Linder S. Metalloproteinase MT1-MMP islets act as memory devices for podosome reemergence. *J Cell Biol*. 2016;**213**:109–25.
- 36 Jackson HW, Defamie V, Waterhouse P, Khokha R. TIMPs: versatile extracellular regulators in cancer. *Nat Rev Cancer*. 2017;**17**:38–53.
- 37 Hahn D, Pischitzis A, Roesmann S, Hansen MK, Leuenberger B, Luginbuehl U, et al. Phorbol 12-myristate 13-acetate-induced ectodomain shedding and phosphorylation of the human meprin beta metalloprotease. *J Biol Chem*. 2003;**278**:42829–39.
- 38 Itoh Y, Takamura A, Ito N, Maru Y, Sato H, Suenaga N, et al. Homophilic complex formation of MT1-MMP facilitates proMMP-2 activation on the cell surface and promotes tumor cell invasion. *EMBO J*. 2001;**20**:4782–93.
- 39 Knauper V, Will H, Lopez-Otin C, Smith B, Atkinson SJ, Stanton H, et al. Cellular mechanisms for human

- procollagenase-3 (MMP-13) activation. Evidence that MT1-MMP (MMP-14) and gelatinase a (MMP-2) are able to generate active enzyme. *J Biol Chem*. 1996;**271**:17124–31.
- 40 Antczak C, Radu C, Djaballah H. A profiling platform for the identification of selective metalloprotease inhibitors. *J Biomol Screen*. 2008;**13**:285–94.
- 41 Thul PJ, Akesson L, Wiking M, Mahdessian D, Geladaki A, Ait Blal H, et al. A subcellular map of the human proteome. *Science*. 2017;**356**:eaal3321.
- 42 Tucher J, Linke D, Koudelka T, Cassidy L, Tredup C, Wichert R, et al. LC-MS based cleavage site profiling of the proteases ADAM10 and ADAM17 using proteome-derived peptide libraries. *J Proteome Res*. 2014;**13**:2205–14.
- 43 Eckhard U, Huesgen PF, Schilling O, Bellac CL, Butler GS, Cox JH, et al. Active site specificity profiling of the matrix metalloproteinase family: proteomic identification of 4300 cleavage sites by nine MMPs explored with structural and synthetic peptide cleavage analyses. *Matrix Biol*. 2016;**49**:37–60.
- 44 Hikita A, Yana I, Wakeyama H, Nakamura M, Kadono Y, Oshima Y, et al. Negative regulation of osteoclastogenesis by ectodomain shedding of receptor activator of NF-kappaB ligand. *J Biol Chem*. 2006;**281**:36846–55.
- 45 Kadono Y, Shibahara K, Namiki M, Watanabe Y, Seiki M, Sato H. Membrane type 1-matrix metalloproteinase is involved in the formation of hepatocyte growth factor/scatter factor-induced branching tubules in madin-Darby canine kidney epithelial cells. *Biochem Biophys Res Commun*. 1998;**251**:681–7.
- 46 Belien AT, Paganetti PA, Schwab ME. Membrane-type 1 matrix metalloprotease (MT1-MMP) enables invasive migration of glioma cells in central nervous system white matter. *J Cell Biol*. 1999;**144**:373–84.
- 47 Lottaz D, Hahn D, Muller S, Muller C, Sterchi EE. Secretion of human meprin from intestinal epithelial cells depends on differential expression of the alpha and beta subunits. *Eur J Biochem*. 1999;**259**:496–504.
- 48 Beynon RJ, Shannon JD, Bond JS. Purification and characterization of a metallo-endoproteinase from mouse kidney. *Biochem J*. 1981;**199**:591–8.
- 49 Becker-Pauly C, Howel M, Walker T, Vlad A, Aufvenne K, Oji V, et al. The alpha and beta subunits of the metalloprotease meprin are expressed in separate layers of human epidermis, revealing different functions in keratinocyte proliferation and differentiation. *J Invest Dermatol*. 2007;**127**:1115–25.
- 50 Hou S, Diez J, Wang C, Becker-Pauly C, Fields GB, Bannister T, et al. Discovery and optimization of selective inhibitors of Meprin alpha (part I). *Pharmaceuticals (Basel)*. 2021;**14**:197.
- 51 Minond D. Novel approaches and challenges of discovery of exosite modulators of a Disintegrin and metalloprotease 10. *Front Mol Biosci*. 2020;**7**:75.
- 52 Chan KM, Wong HL, Jin G, Liu B, Cao R, Cao Y, et al. MT1-MMP inactivates ADAM9 to regulate FGFR2 signaling and calvarial osteogenesis. *Dev Cell*. 2012;**22**:1176–90.
- 53 Tousseyn T, Thathiah A, Jorissen E, Raemaekers T, Konietzko U, Reiss K, et al. ADAM10, the rate-limiting protease of regulated intramembrane proteolysis of notch and other proteins, is processed by ADAMS-9, ADAMS-15, and the gamma-secretase. *J Biol Chem*. 2009;**284**:11738–47.
- 54 Holmbeck K, Bianco P, Caterina J, Yamada S, Kromer M, Kuznetsov SA, et al. MT1-MMP-deficient mice develop dwarfism, osteopenia, arthritis, and connective tissue disease due to inadequate collagen turnover. *Cell*. 1999;**99**:81–92.
- 55 Schjoldager KT, Clausen H. Site-specific protein O-glycosylation modulates proprotein processing – deciphering specific functions of the large polypeptide GalNAc-transferase gene family. *Biochim Biophys Acta*. 2012;**1820**:2079–94.
- 56 Goth CK, Halim A, Khetarpal SA, Rader DJ, Clausen H, Schjoldager KT. A systematic study of modulation of ADAM-mediated ectodomain shedding by site-specific O-glycosylation. *Proc Natl Acad Sci USA*. 2015;**112**:14623–8.
- 57 Leuenberger B, Hahn D, Pischitzis A, Hansen MK, Sterchi EE. Human meprin beta: O-linked glycans in the intervening region of the type I membrane protein protect the C-terminal region from proteolytic cleavage and diminish its secretion. *Biochem J*. 2003;**369**:659–65.
- 58 Tate JG, Bamford S, Jubb HC, Sondka Z, Beare DM, Bindal N, et al. COSMIC: the catalogue of somatic mutations in cancer. *Nucleic Acids Res*. 2019;**47**:D941–7.
- 59 Hedrich J, Lottaz D, Meyer K, Yiallourous I, Jahn-Dechent W, Stocker W, et al. Fetuin-a and cystatin C are endogenous inhibitors of human meprin metalloproteases. *Biochemistry*. 2010;**49**:8599–607.
- 60 Becker C, Kruse MN, Slotty KA, Kohler D, Harris JR, Rosmann S, et al. Differences in the activation mechanism between the alpha and beta subunits of human meprin. *Biol Chem*. 2003;**384**:825–31.
- 61 Broder C, Becker-Pauly C. The metalloproteases meprin alpha and meprin beta: unique enzymes in inflammation, neurodegeneration, cancer and fibrosis. *Biochem J*. 2013;**450**:253–64.
- 62 Perez-Riverol Y, Bai J, Bandla C, Garcia-Seisdedos D, Hewapathirana S, Kamatchinathan S, et al. The PRIDE database resources in 2022: a hub for mass spectrometry-based proteomics evidences. *Nucleic Acids Res*. 2022;**50**:D543–52.